Ultrasonics 77 (2017) 61–68

Contents lists available at ScienceDirect

Ultrasonics

journal homepage: www.elsevier.com/locate/ultras

Electroless deposition of nickel-boron coatings using low frequency ultrasonic agitation: Effect of ultrasonic frequency on the coatings

L. Bonin [a,*], N. Bains [b], V. Vitry [a], A.J. Cobley [b]

[a] Metallurgy Lab, UMONS, 20 place du Parc, 7000 Mons, Belgium
[b] The Functional Materials Research Group, Centre for Manufacturing and Materials Engineering, Faculty of Engineering, The Environment and Computing, Coventry University, Priory Street, Coventry CV1 5FB, UK

ARTICLE INFO

Article history:
Received 20 September 2016
Received in revised form 14 December 2016
Accepted 25 January 2017
Available online 30 January 2017

Keywords:
Electroless deposition
Nickel-boron
Sonochemistry
Ultrasound agitation

ABSTRACT

The effect of ultrasound on the properties of Nickel-Boron (NiB) coatings was investigated. NiB coatings were fabricated by electroless deposition using either ultrasonic or mechanical agitation. The deposition of Ni occurred in an aqueous bath containing a reducible metal salt (nickel chloride), reducing agent (sodium borohydride), complexing agent (ethylenediamine) and stabilizer (lead tungstate). Due to the instability of the borohydride in acidic, neutral and slightly alkaline media, pH was controlled at pH 12 ± 1 in order to avoid destabilizing the bath. Deposition was performed in three different configurations: one with a classical mechanical agitation at 300 rpm and the other two employing ultrasound at a frequency of either 20 or 35 kHz. The microstructures of the electroless coatings were characterized by a combination of optical Microscopy and Scanning Electron Microscope (SEM). The chemistry of the coatings was determined by ICP-AES (Inductively Coupled Plasma - Atomic Emission Spectrometry) after dissolution in aqua regia. The mechanical properties of the coatings were established by a combination of roughness measurements, Vickers microhardness and pin-on-disk tribology tests. Lastly, the corrosion properties were analysed by potentiodynamic polarization. The results showed that low frequency ultrasonic agitation could be used to produce coatings from an alkaline NiB bath and that the thickness of coatings obtained could be increased by over 50% compared to those produced using mechanical agitation. Although ultrasonic agitation produced a smoother coating and some alteration of the deposit morphology was observed, the mechanical and corrosion properties were very similar to those found when using mechanical agitation.

1. Introduction

Seventy years after the discovery of electroless Ni by Brenner and Riddell in 1946 [1], the electroless deposition process underwent several modifications to meet the challenging needs of a variety of industrial applications. Electroless deposited Ni coatings have been widely used in different industries such as electronics, automotive, aerospace, medical, petrochemical, food and military etc. This wide field of application can be explained by a well-known combination of properties, including high corrosion resistance, excellent wear resistance, uniformity of coating thickness and magnetic properties [2–9].

Nickel alloys obtained by electroless deposition are categorized according to their alloying elements. The most widely used and studied alloy is nickel–phosphorous (NiP), which is obtained using sodium hypophosphite as the reducing agent. Electroless NiB alloys (that have borohydride ion or amine–borane compounds as the reducing agent) are the second most used electroless Ni alloy, possessing very interesting properties that support industrial requirements. When compared with NiP coatings, electroless NiB deposits present a much higher hardness (up to 900 hv_{100} against 500–700 hv_{100}) [10], have better wear and scratch resistances and promising electrical behaviour [11–21].

Compared with electrodeposited Ni coatings, electroless NiB is far superior regarding uniform plating thickness distribution. This is an important factor when plating components with complex shapes and miniaturised features. In addition, electroless NiB composite deposits might present higher corrosion resistance, superior mechanical properties and the ability to be deposited on a much wider range of materials, such as dielectric substrates (important for electronic applications).

Sonochemistry has attracted much interest in the research community because of its broad application in materials engineering.

* Corresponding author.
E-mail address: luiza.bonin@umons.ac.be (L. Bonin).

http://dx.doi.org/10.1016/j.ultras.2017.01.021
0041-624X/

Ultrasonically assisted Ni plating can alter the chemical and physical properties of electrolytic Ni and electroless Ni deposits. The addition of an acoustic field has been shown to promote beneficial effects on electrochemical processes in general [22–28,24,29] and electroless deposition in particular [30–39,30,31]. The use of ultrasound in electrochemical processes has been reported to improve the electrodeposition process itself as well as the characteristics of Ni deposits. Previous studies have indicated that ultrasonic agitation can increase the deposition rate [24,32,34,40,41] and increase the deposit hardness [24,25,28,34]. Other studies have shown that the acoustic field tends to decrease the residual stress [25,28] and enhance the wear resistance [28] and adhesion of the deposit to the samples [24,33]. In addition, a reduction of porosity has been observed [41,42].

While there are a number of studies concerning ultrasonically assisted methods for electrolytic Ni deposition [28,32,43,44] and others that have investigated the use of ultrasound in electroless NiP plating [45–49], there are only a few studies about the addition of ultrasound in electroless NiB coatings [43,50]. In addition, the previous studies concerning the creation of ultrasonically assisted NiB coatings were developed mainly for baths using amineborane compounds rather than sodium borohydride. The aim of this preliminary study is to develop ultrasound assisted NiB coatings reduced by borohydride to improve the properties of alkaline NiB plating. Electroless NiB is described in the literature as a high performance coating, however price of the chemicals used in the process are relatively expensive and this makes it less popular than other coatings in the industry. This work aims to increase the plating rate with the addition of ultrasound in the bath, in order to decrease production time and cost.

Ultrasound (20 kHz and 35 kHz frequency) was employed to agitate NiB electroless solutions to produce NiB coatings on mild steel. The microstructures, hardness, wear and corrosion resistances of the deposits were compared with mechanically agitated electroless NiB coatings.

2. Experimental procedure

2.1. Preparation of substrate

Mild steel (St-37) samples with dimensions of 25 mm × 25 mm × 1 mm were used as substrates. A hole of 2 mm in diameter was drilled in the border of one edge of each specimen for convenient hanging in the solution during plating. The substrates were prepared by mechanical grinding with SiC paper of 180, 500, and 1200 grit. After this process, the samples were cleaned and degreased with acetone. Just before plating, the samples were activated by etching in 32 vol.% hydrochloric acid for 3 min, directly followed by rinsing in flowing distilled water and immersion in the electroless Ni-B solution.

2.2. Electroless nickel baths

Electroless plating baths (500 ml) were prepared on a regulated hot plate (95 ± 1 °C) with magnetic stirring. The NiB bath was composed of sodium borohydride ($NaBH_4$) as reducing agent, nickel chloride hexahydrate ($NiCl_2{\cdot}6H_2O$) as nickel source, ethylenediamine ($NH_2–CH_2–CH_2–NH_2$) as complexing agent and lead tungstate ($PbWO_4$) as stabilizer. The bath pH was 12 ± 1. The precise bath composition is presented in Table 1.

2.3. Bath agitation

Three different methods of bath agitation were used during the plating process. The first (= classical) was a mechanical agitation generated by magnetic stirring while the temperature was maintained at 95 °C by a temperature regulated hot plate. For the second one, the agitation was generated by an ultrasonic probe with a frequency of 20 kHz and a power of 0.058 W/cm^3, estimated by the calorimetric method [26], with the temperature maintained once again at 95 °C by a temperature regulated hot plate. The third procedure consisted of a bath agitated by ultrasound at 35 kHz and 0.065 W/cm^3 of power while the temperature was kept at 95 °C by a thermostated water bath. Therefore for both the ultrasonically agitated solutions the power density used was approximately the same meaning that the main effect was ultrasonic frequency. In all three cases, the preparation of bath was carried out on a hot plate with mechanical agitation generated by magnetic stirring. Fig. 1 clarifies the methods employed for bath preparation and plating process.

Table 1
Bath composition of sodium borohydride reduced electroless Ni bath.

Nickel chloride	24 g/l
Sodium hydroxide	39 g/l
Ethylenediamine $NH_2CH_2CH_2NH_2$	60 ml/l
Lead tungstate	0.021 g/l
Sodium borohydride	0.602 g/l

2.4. Coating characterization

A Scanning Electron Microscope (Hitachi's SU8200) was used to study the cross morphology through a section of the coating, while the surface morphology was analysed by a HIROX KH-8700 Digital Optical Microscope.

In order to obtain the overall composition of the deposits, the samples were dissolved in aqua regia (1/3 nitric acid - 2/3 hydrochloric acid) and the resulting solutions were analysed by ICP-AES (inductively coupled plasma - atomic emission spectrometry).

Roughness measurements were carried out using a Zeiss 119SURFCOM 1400D-3DF. A Microhardness tester (Mitutoyo HM-200) equipped with Koop indenter was employed for hardness measuring. Hardness measurements were carried out on the specimens' cross sections under a load of 100 gf and load exertion time of 20 s.

The tribological behaviour of the samples was investigated using a pin-on-disk CSM microtribometer (without the use of lubricants) where the coated samples served as the disks and the counterparts were 6 mm diameter alumina balls with hardness of 1400 HV. The sliding speed and sliding distance were, respectively, 12 cm/s and 200 m. Wear tests were carried out under normal loads of 10 N, at 20 °C and with 45% humidity.

Bio-logic SP-50 equipment was used in this study to obtain potentiodynamic polarization curves in 0.1 M NaCl solution. The tests were performed in a standard three-electrode cell. Platinum plate and Ag/AgCl (KCl saturated) electrode were used as counter and reference electrodes, respectively. Before the polarization analysis a 20 min OCP was applied. A potential range of ±0.6 V Vs OCP, at 1 mV/s scan rate, was employed.

3. Experimental results and discussion

3.1. Structural and morphological characterization

Surface observation of the coatings by optical microscope (Fig. 2) shows the typical cauliflower-like texture for mechanically agitated electroless NiB coatings (a). The surface texture of NiB coatings produced using 20 kHz ultrasonic agitation has a similar structure but visually appears smoother. However when 35 kHz

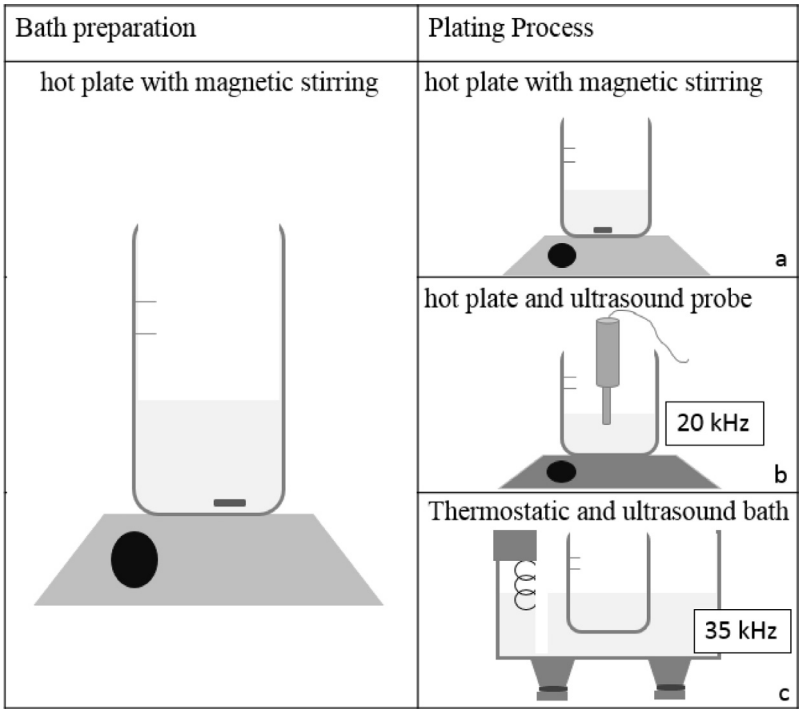

Fig. 1. Bath preparation and plating process agitation methods.

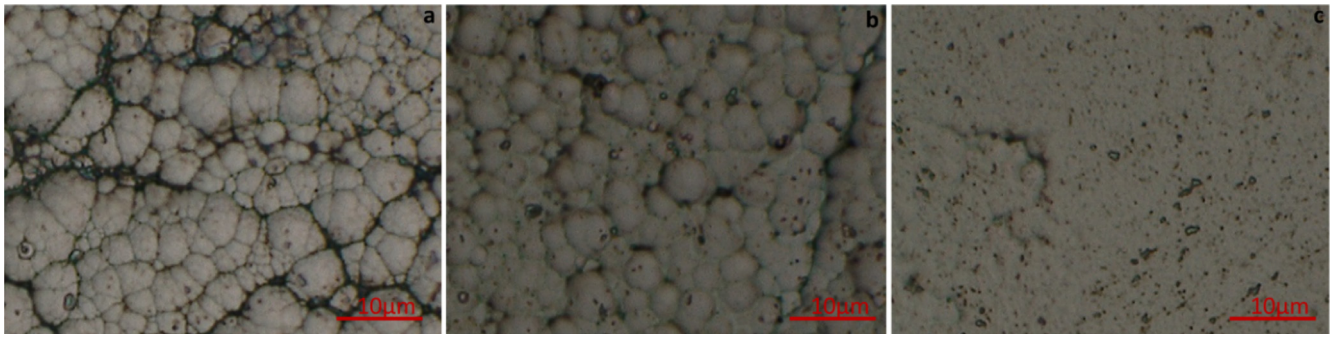

Fig. 2. Optical microscope surface morphology (a) electroless NiB without ultrasound, (b) electroless NiB with 20 kHz frequency and 0.058 W/cm^3 energy density ultrasound, (c) electroless NiB with 35 kHz frequency and 0.065 W/cm^3 energy density ultrasound.

ultrasound is utilised for agitation the coatings produced show a significant change in surface structure: the texture is not very prominent and the morphology becomes quite smooth. However, some small residual areas still present a slight cauliflower-like texture.

Cross section observation by SEM (Fig. 3) shows the formation of columnar morphology for all samples. However, the ultrasound-assisted samples present finer, probably denser, morphology. Rao et al. [51] have observed the formation of electroless NiB deposits in a non-replenished and non-agitated bath. They observed that the typical columnar morphology of electroless NiB deposits was related to the diffusion of reactive species in the bath. When the bath became depleted in reactive species a thick diffusion layer near the deposits was generated, that would then slow the growth of the columns and induce a new germination phase leading to the nodular layer.

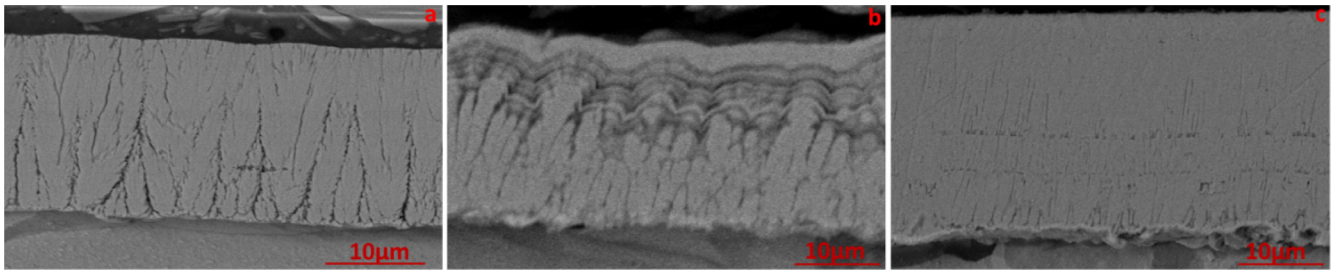

Fig. 3. SEM cross section morphology (a) electroless NiB without ultrasound, (b) electroless NiB with 20 kHz frequency and 0.058 W/cm^3 energy density ultrasound, (c) electroless NiB with 35 kHz frequency and 0.065 W/cm^3 energy density ultrasound.

In this case, the utilization of ultrasound, instead of mechanical agitation, has generated an improvement in the deposition efficiency (increased plating rate, see Table 2). A higher deposition efficiency might have caused the depletion of reactive species in the bath, leading to new germination phases and to a denser layer.

The denser appearance could also be explained by the absence of hydrogen gas occlusion. The deposition mechanism of electroless Ni involves generation of hydrogen which can be entrapped in the NiB layer [52]. High power ultrasound is well known for its ability to degas solutions and therefore may results in a decrease of entrapped hydrogen in the coating [53].

As shown in Table 2, the coatings produced using ultrasonic agitation are thicker than if mechanical agitation is employed. Considering that all coatings have the same plating time (1 h), it can be deduced that the use of ultrasound increases the bath plating rate. Therefore, the application of an acoustic field increases the plating efficiency.

3.2. Chemical composition

A knowledge of the chemical composition of the electroless coating is important because it can influence its other properties. To obtain the overall composition of the deposits, the samples were dissolved in aqua regia and analysed by ICP. Table 3 indicates that, the compositions of the samples are in the same range, on average containing approximately 6 wt.% boron and 1 wt.% lead with the balance being nickel (93 wt.%). The slight variations between coatings could be due to minor changes in the bath temperature caused by the ultrasound agitation. Further investigation will be necessary to determine if sonication promotes the deposition of specific elements.

3.3. Mechanical properties

In order to analyse the surface finish of the samples, three roughness parameters were used: Ra (Average roughness, arithmetic mean of the distances to the median), Rp (Peak roughness, amplitude of the highest peak within the scan length) and Rv (Valley roughness, amplitude of the highest valley within the scan length).

Roughness values are presented in Table 4. As expected according to the surface morphology analyses, Ra decreases in the case of ultrasound assisted baths. The low values of Rp achieved are also quite meaningful i.e. it suggests there were no Ni microparticles stuck to the sample surface (this phenomenon is likely to occur when the plating bath is becoming unstable). Rv values are also low, indicating the absence of deep holes in the coatings.

Vickers microhardness values were measured in polished cross sections of the coatings. The values achieved are all in the same range. However, the use of 20 kHz frequency ultrasound in the electroless solution seems to slightly decrease the coating hardness. This is probably due to a greater elimination of hydrogen, thereby, decreasing the internal stress and making the coatings more ductile and less hard. Compressive stresses can occur when codeposited gases, such as hydrogen, diffuse into microvoids and expand them [54].

Table 2
Measured thickness, electroless NiB without ultrasound, electroless NiB with 20 kHz frequency ultrasound and electroless NiB with 35 kHz frequency ultrasound.

Samples	Thickness (μm)
NiB without ultrasound	16.22 ± 0.59
NiB 20 hKz	23.03 ± 1.95
NiB 35 hKz	25.13 ± 2.02

Table 3
Chemical composition of the electroless coating using either mechanical or ultrasonic agitation.

Samples	Ni (wt.%)	B (wt.%)	Pb (wt.%)
NiB without ultrasound	93.01	5.92	1.05
NiB 20 kHz	92.55	6.11	1.33
NiB 35 kHz	93.76	5.47	0.75

3.4. Pin-on-disk tribology test

The coefficient of friction indicates the ease of sliding between two surfaces. As one can perceive in Table 5, the coefficient of friction decreases when the bath is agitated by ultrasound.

The specific wear rate (Ws) was calculated following the European standard EN 1017-13:2008, where Ws is the volume wear loss ΔV, divided by the applied load F_N and the sliding distance S. The best wear behaviours are associated with lower values of Ws.

Assuming that wear resistance is related to hardness, one might suppose that tribological behaviour of all samples would be in the same range, with a slight decrease in the resistance in the case of coatings produced under 20 kHz ultrasonic agitation. In fact this is virtually what is found, although the wear resistance is highest for NiB coatings produced without ultrasound, followed by those coatings produced using ultrasonic agitation at 35 kHz. The coatings produced using 20 kHz ultrasonic agitation had the lowest values of wear resistance. However it should be stated that the wear resistance stays in the same range for the coatings produced whatever the method of agitation.

Further analysis carried out on the worn surfaces of the coatings after the pin-on-disk test was performed by means of optical microscopy (Fig. 4) and showed how wear marks are wider when the hardness is lower. This fact is due to the ease with which material is removed from the softer surfaces. A more adherent coating will also increase the wear behaviour. Although the wear resistance values of the tree different coatings are in the same range, the analysis of wear tracks reveals slightly varied wear behaviours. NiB coatings produced by mechanical agitation (a) and NiB coatings produced using 35 kHz frequency ultrasonic agitation (c) present similar mechanisms of abrasive and adhesive wear, due to the combination of high hardness and ductility, with a dominance of abrasiveness. Considering the NiB coatings produced under 20 kHz frequency ultrasonic agitation (b), combined abrasive and adhesive wear is also observed. However, in this case, adhesive wear predominates due to the lower values of hardness and ductility. Surface analysis on the alumina balls (Fig. 5) shows that a significant amount of the NiB coatings produced using 20 kHz agitation (Fig. 5b) has been transferred to the ball (high ductility).

3.5. Corrosion

Results of potentiodynamic polarization tests are presented in Fig. 6. The tests were performed for the coating produced using the three different agitation systems on a mild steel (substrate) in 0.1 M NaCl solution. When compared to the bare steel, all the coated samples (a, b, c) present a better behaviour: a positive shift in the corrosion potentials (E_{corr}) and a decrease in the corrosion current densities (i_{corr}). Indeed, all coatings present an i_{corr} about 2 orders of magnitude lower than the bare steel. The difference in polarization behaviour between the coatings and the mild steel suggests that the deposited layers completely cover the substrate [55].

Undoubtedly, differences exist in the surface area of the samples and, in fact, this trend is revealed by the observed differences in the rate of the cathodic reactions; namely, the reduction of

Table 4
Roughness Ra and Rp values and Vickers microhardness, electroless NiB without ultrasound, electroless NiB with 20 kHz frequency ultrasound and electroless NiB with 35 kHz frequency ultrasound.

Samples	R_a (μm)	R_v (μm)	R_p (μm)	Hardness H_{V100}
NiB without ultrasound	0.71 ± 0.07	3.03 ± 0.49	2.69 ± 0.37	842.72 ± 52
NiB 20 kHz	0.39 ± 0.13	2.00 ± 0.44	1.95 ± 0.45	750.97 ± 38
NiB 35 kHz	0.35 ± 0.03	1.66 ± 0.20	1.84 ± 0.82	844.32 ± 31

Table 5
Pin-on-disk coefficient of friction, wear tracks thickness and specific wear rate Ws of NiB coatings produced using either mechanical or ultrasonic agitation.

Samples	Friction coefficient u	Wear tracks width (μm)	Specific wear rate Ws ($\mu m^2/N$)
NiB without ultrasound	0.513	370 ± 2	0.41
NiB 20 kHz	0.468	385 ± 5	0.46
NiB 35 kHz	0.451	376 ± 5	0.43

oxygen and the evolution of hydrogen (at more negative potentials). In agreement with the surface morphology results, the polarization curves reveal that the higher the surface area, the higher the cathodic current densities: coating (a), which has the highest surface area, presents the highest rates of cathodic reactions, while coating (c) (surface area comparable to the bare substrate) presents the lowest cathodic reactions rates.

Even if the coatings present (in general) higher surface area than the bare substrate, they yield much lower anodic reactions suggesting that, indeed, anodic dissolution is greatly reduced in the case of the coated systems.

Due to these dissimilar surface areas issue, a direct comparison of current density values from different coatings is not straightforward. For that reason, when comparing the different systems, the authors have restricted the discussion to the differences in shape (presence of plateau) of the anodic curves. Comparing the anodic polarization curves, the shape for the bare steel is similar to the shape for sample (a), while the curves for the coatings produced using ultrasonic agitation present one (c) or two (b) current density plateaux. These plateaux might indicate that a passive state is temporarily reached for those systems. The passive-transpassive behaviour is often observed for NiP coatings (that are known for their superior anti-corrosion properties [56]). Chemical composition (in particular, B content [55]) along with morphological parameters (coating thickness, roughness) have a great impact on the corrosion behaviour.

The corrosion potential Ecorr is independent of the surface area. The increase of the Ecorr in the presence of coatings can then be attributed to presence of the coating on the steel surface (Ni is nobler than Fe). Moreover, the chemical nature of the surface also has a considerable effect on the kinetics of reduction reactions. This fact may also explain the variations in the hydrogen evolution potential observed for the different systems.

The passive film of nickel is susceptible to pitting corrosion in the presence of chlorides [57]. Furthermore, in the present case, the deposition of Ni atoms leads to the generation of a considerable amount of boundaries (especially in the absence of US). These boundaries, such as grain boundaries and column boundaries, create conditions for intergranular and intercolumnar corrosion to take place. Therefore, the coated system should be particularly susceptible to localized corrosion processes. Fig. 7 shows the surface morphology for the different samples after polarization tests.

Concerning coating (a), the SEM analysis after the polarization test (Fig. 7(a)) shows that significant pitting (grooves with corrosion product rings around them) as well as intergranular corrosion took place. According to the polarization curve of sample (a), both localized corrosion processes appear to have proceeded simultaneously, as the slope of the anodic reaction is quite sharp and no plateau is observed.

With respect to the anodic curve from coating (b), it clearly presents 2 plateaus followed by 2 breakdown potentials: first, intergranular corrosion takes place and, at more positive potentials, pitting is evidenced. The fact that this microstructure presents much less boundaries (compared to coating (a)) explains why both localized mechanisms may be distinguished. From the SEM micrograph (b), corrosion products can be seen on both the bulk of columns as well as on the boundaries. The SEMs also appear to show that corrosion has happened to a much lower extent than in sample (a).

Regarding coating (c), the anodic polarization curve reveals the presence of a large plateau preceding the pitting potential. This may be a consequence of the quite smooth surface obtained in this case, which limits the occurrence of intercolumnar attack. As the SEM micrographs after polarization tests indicate, the surface of coating (c) presented much less corrosion damage than coating (a), with pitting being the main mechanism of corrosion.

In order to gather more insights on corrosion properties of the coatings, further electrochemical studies will be performed in the future.

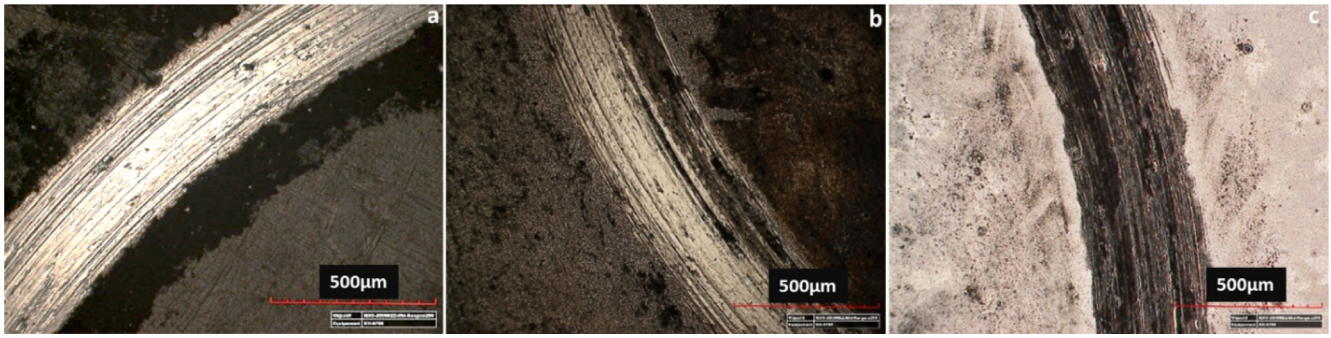

Fig. 4. Optical microscope surface of wear tracks (a) electroless NiB without ultrasound, (b) electroless NiB with 20 kHz frequency and 0.058 W/cm^3 energy density ultrasound, (c) electroless NiB with 35 kHz frequency and 0.065 W/cm^3 energy density ultrasound.

Fig. 5. Optical microscope surface of testing alumina balls after the dry sliding friction test. (a) Electroless NiB without ultrasound, (b) electroless NiB with 20 kHz frequency and 0.058 W/cm^3 energy density ultrasound, (c) electroless NiB with 35 kHz frequency and 0.065 W/cm^3 energy density ultrasound.

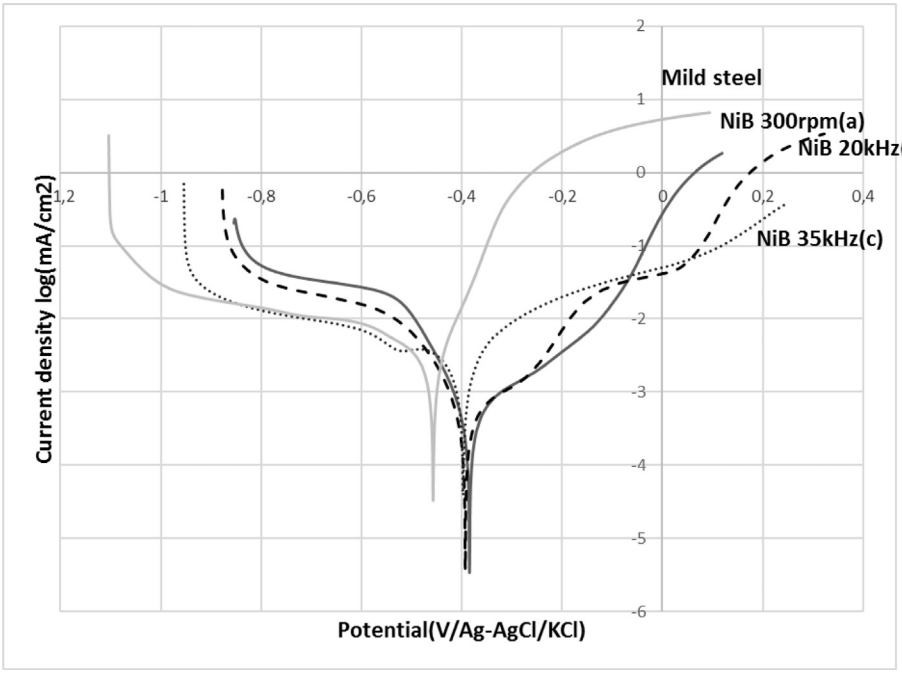

Fig. 6. Potentiodynamic polarization curves, 0.1 M NaCl, (a) electroless NiB without ultrasound, (b) electroless NiB with 20 kHz frequency and 0.058 W/cm^3 energy density ultrasound, (c) electroless NiB with 35 kHz frequency and 0.065 W/cm^3 energy density ultrasound.

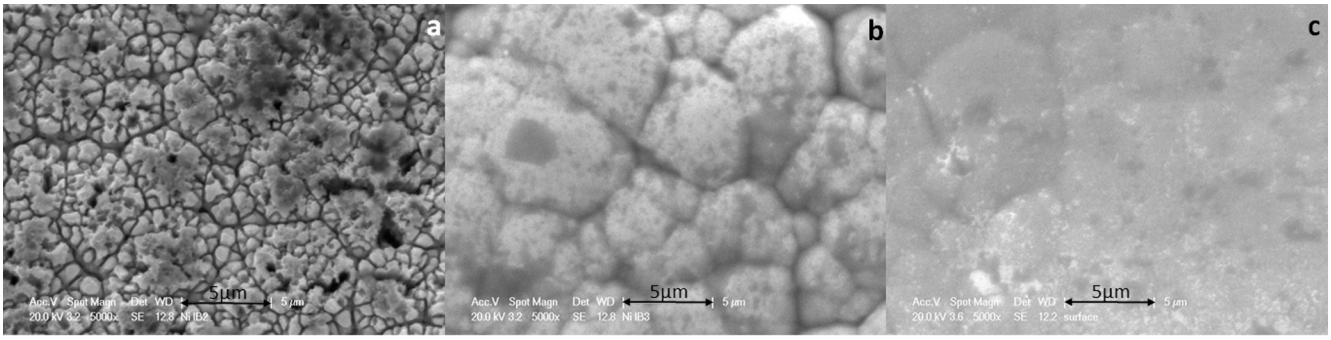

Fig. 7. SEM surface morphology after polarization tests (a) electroless NiB without ultrasound, (b) electroless NiB with 20 kHz frequency and 0.058 W/cm^3 energy density ultrasound, (c) electroless NiB with 35 kHz frequency and 0.065 W/cm^3 energy density ultrasound.

4. Conclusions

In view of improving the already interesting properties of electroless NiB coatings, an ultrasonic probe and ultrasonic bath were employed to agitate the plating solution to produce Ni-B coatings on mild steel. These were characterised and compared to electroless Ni-B coatings produced using a classical mechanically agitated solution.

The morphology of the coatings without ultrasound was in agreement with the literature i.e. a cauliflower-like surface texture was observed and a columnar cross section. In the case of coatings produced under ultrasonic agitation, the surface was smoother and less porous (as shown by the cross section analysis). As expected, based on the surface morphology analyses, the roughness decreased in the case of ultrasound assisted baths.

Regarding the mechanical properties, the use of ultrasound did not bring significant modification of the hardness or wear behaviour. However, significant differences in pitting potential are observable on the polarization curves and beneficial effects of ultrasound assistance can be seen.

The main advantage observed with ultrasonic agitation was a significant increase of the plating rate. When ultrasonic agitation was employed the coating thickness increased by over 50%. This is an important finding since industry demands higher plating speeds, reduced production times and enhanced material properties. The results from this study suggest that the use of ultrasound to agitate electroless NiB solutions has the potential to fulfil these requirements.

Acknowledgments

One of the authors (L. Bonin) wishes to thank the CNPq (Conselho Nacional de Desenvolvimento Científico e Tecnológico) for funding.

References

[1] A. Brenner, G.E. Riddell, Nickel plating on steel by chemical reduction, J. Res. Natl. Bur. Stand. 37 (1946) (1934) 31, http://dx.doi.org/10.6028/jres.037.019.
[2] F. Bigdeli, S.R. Allahkaram, An investigation on corrosion resistance of as-applied and heat treated Ni-P/nanoSiC coatings, Mater. Des. 30 (2009) 4450–4453, http://dx.doi.org/10.1016/j.matdes.2009.04.020.
[3] M. Franco, W. Sha, G. Aldic, S. Malinov, H. Çimenoğlu, Effect of reinforcement and heat treatment on elevated temperature sliding of electroless Ni–P/SiC composite coatings, Tribol. Int. 97 (2016) 265–271, http://dx.doi.org/10.1016/j.triboint.2016.01.047.
[4] A.S. Hamada, P. Sahu, D.A. Porter, Indentation property and corrosion resistance of electroless nickel-phosphorus coatings deposited on austenitic high-Mn TWIP steel, Appl. Surf. Sci. 356 (2015) 1–8, http://dx.doi.org/10.1016/j.apsusc.2015.07.153.
[5] C.K. Lee, Structure, electrochemical and wear-corrosion properties of electroless nickel-phosphorus deposition on CFRP composites, Mater. Chem. Phys. 114 (2009) 125–133, http://dx.doi.org/10.1016/j.matchemphys.2008.08.088.
[6] G. Straffelini, D. Colombo, A. Molinari, Surface durability of electroless Ni-P composite deposits, Wear 236 (1999) 179–188, http://dx.doi.org/10.1016/S0043-1648(99)00273-2.
[7] W. Wang, W. Zhang, Y. Wang, N. Mitsuzak, Z. Chen, Ductile electroless Ni – P coating onto flexible printed circuit board, Appl. Surface Sci. 367 (2016) 528–532.
[8] H. Yang, Y. Gao, W. Qin, Y. Li, Microstructure and corrosion behavior of electroless Ni – P on sprayed Al – Ce coating of 3003 aluminum alloy, Surf. Coatings Technol. 281 (2015) 176–183.
[9] M. Zhang, S. Mu, Q. Guan, W. Li, J. Du, A high anticorrosive chromium-free conversion coating prepared with an alkaline conversion bath on electroless Ni-P coating, Appl. Surf. Sci. 349 (2015) 108–115, http://dx.doi.org/10.1016/j.apsusc.2015.04.209.
[10] V. Vitry, A. Sens, F. Delaunois, Comparison of various electroless nickel coatings on steel: structure, hardness and abrasion resistance, Mater. Sci. Forum. 783–786 (2014) 1405–1413, http://dx.doi.org/10.4028/www.scientific.net/MSF.783-786.1405.
[11] F. Delaunois, P. Lienard, Heat treatments for electroless nickel – boron plating on aluminium alloys, Surf. Coatings Technol. 160 (2002) 239–248, http://dx.doi.org/10.1016/S0257-8972(02)00415-2.
[12] F. Delaunois, J.P. Petitjean, P. Lienard, M. Jacob-Duliere, Autocatalytic electroless nickel-boron plating on light alloys, Surf. Coatings Technol. 124 (2000) 201–209, http://dx.doi.org/10.1016/S0257-8972(99)00621-0.
[13] V. Vitry, F. Delaunois, Formation of borohydride-reduced nickel–boron coatings on various steel substrates, Appl. Surf. Sci. 359 (2015) 692–703, http://dx.doi.org/10.1016/j.apsusc.2015.10.205.
[14] V. Vitry, F. Delaunois, C. Dumortier, How heat treatment can give better properties to electroless nickel-boron coatings, Metall. Ital. 101 (2009).
[15] V. Vitry, F. Delaunois, C. Dumortier, Mechanical properties and scratch test resistance of nickel-boron coated aluminium alloy after heat treatments, Surf. Coatings Technol. 202 (2008) 3316–3324, http://dx.doi.org/10.1016/j.surfcoat.2007.12.001.
[16] V. Vitry, F. Delaunois, Nanostructured electroless nickel-boron coatings for wear resistance, Anti-Abrasive Nanocoatings (2015) 157–199, http://dx.doi.org/10.1016/B978-0-85709-211-3.00007-8.
[17] V. Vitry, A. Sens, A. Kanta, F. Delaunois, Experimental study on the formation and growth of electroless nickel- boron coatings from borohydride-reduced bath on mild steel, (n.d.) 1–21.
[18] T.S.N. Sankara Narayanan, S.K. Seshadri, Formation and characterization of borohydride reduced electroless nickel deposits, J. Alloys Compd. 365 (2004) 197–205, http://dx.doi.org/10.1016/S0925-8388(03)00680-7.
[19] B. Oraon, G. Majumdar, B. Ghosh, Improving hardness of electroless Ni-B coatings using optimized deposition conditions and annealing, Mater. Des. 29 (2008) 1412–1418, http://dx.doi.org/10.1016/j.matdes.2007.09.005.
[20] K.H. Lee, D. Chang, S.C. Kwon, Properties of electrodeposited nanocrystalline Ni-B alloy films, Electrochim. Acta 50 (2005) 4538–4543, http://dx.doi.org/10.1016/j.electacta.2004.03.067.
[21] K. Krishnaveni, T.S.N. Sankara Narayanan, S.K. Seshadri, Electroless Ni-B coatings: preparation and evaluation of hardness and wear resistance, Surf. Coatings Technol. 190 (2005) 115–121, http://dx.doi.org/10.1016/j.surfcoat.2004.01.038.
[22] A. Chiba, T. Gotou, K. Kobayashi, W.C. Wu, Influence of sonication of nickel plating in a nickel sulfamate bath, Metal Finish. (2000).
[23] F. Su, C. Liu, P. Huang, Ultrasound-assisted pulse electrodeposition and characterization of Co–W/MWCNTs nanocomposite coatings, Appl. Surf. Sci. 309 (2014) 200–208, http://dx.doi.org/10.1016/j.apsusc.2014.05.010.
[24] M.E. Hyde, R.G. Compton, How ultrasound influences the electrodeposition of metals, J. Electroanal. Chem. 531 (2002) 19–24, http://dx.doi.org/10.1016/S0022-0728(02)01016-1.
[25] P.B.S.N.V. Prasad, R. Vasudevan, S.K. Seshadri, S. Ahila, The effect of ultrasonic vibration on nickel electrodeposition, Mater. Lett. 17 (1993) 357–359, http://dx.doi.org/10.1016/0167-577X(93)90125-H.
[26] M.K. Camargo, I. Tudela, U. Schmidt, A.J. Cobley, A. Bund, Ultrasound assisted electrodeposition of Zn and Zn-TiO_2 coatings, Electrochim. Acta 198 (2016) 287–295, http://dx.doi.org/10.1016/j.electacta.2016.03.078.
[27] I. Tudela, Y. Zhang, M. Pal, I. Kerr, A.J. Cobley, Ultrasound-assisted electrodeposition of composite coatings with particles, Surf. Coatings Technol. 259 (2014) 363–373, http://dx.doi.org/10.1016/j.surfcoat.2014.06.023.
[28] I. Tudela, Y. Zhang, M. Pal, I. Kerr, T.J. Mason, A.J. Cobley, Ultrasound-assisted electrodeposition of nickel: Effect of ultrasonic power on the characteristics of thin coatings, Surf. Coatings Technol. 264 (2015) 49–59, http://dx.doi.org/10.1016/j.surfcoat.2015.01.020.
[29] T.J. Mason, J.P. Lorimer, D.J. Walton, Sonoelectrochemistry, Ultrasonics 28 (1990).
[30] F. Touyeras, J.Y. Hihn, M.L. Doche, X. Roizard, Electroless copper coating of epoxide plates in an ultrasonic field, Ultrason. Sonochem. 8 (2001) 285–290, http://dx.doi.org/10.1016/S1350-4177(01)00090-6.
[31] Y. Zhao, C. Bao, R. Feng, Z. Chen, Electroless coating of copper on ceramic in an ultrasonic field, Ultrason. Sonochem. 2 (1995) 99–103, http://dx.doi.org/10.1016/1350-4177(94)00011-G.
[32] K. Kobayashi, A. Chiba, N. Minami, Effects of ultrasound on both electrolytic and electroless nickel depositions, Ultrasonics 38 (2000) 676–681, http://dx.doi.org/10.1016/S0041-624X(99)00215-2.
[33] A.J. Cobley, T.J. Mason, V. Saez, Review of effect of ultrasound on electroless plating process, Trans. Inst. Met. Finish. 89 (2011) 303–309, http://dx.doi.org/10.1179/174591911X13170500147670.
[34] Y.S. Park, T.H. Kim, M.H. Lee, S.C. Kwon, Study on the effect of ultrasonic waves on the characteristics of electroless nickel deposits from an acid bath, Surf. Coatings Technol. 153 (2002) 245–251, http://dx.doi.org/10.1016/S0257-8972(01)01683-8.
[35] A.J. Cobley, V. Saez, The use of ultrasound to enable low temperature electroless plating, Circuit World. 38 (2012) 12–15, http://dx.doi.org/10.1108/03056121211195003.
[36] A.J. Cobley, J.E. Graves, B. Mkhlef, B. Abbas, T.J. Mason, Ultrasonically enabled low temperature electroless plating for sustainable electronic manufacture, in: 2012 4th Electron. Syst. Technol. Conf. ESTC 2012, 2012, http://dx.doi.org/10.1109/ESTC.2012.6542132.
[37] J.E. Graves, M. Sugden, R.E. Litchfield, D.A. Hutt, T.J. Mason, A.J. Cobley, Ultrasound assisted dispersal of a copper nanopowder for electroless copper activation, Ultrason. Sonochem. 29 (2016) 428–438, http://dx.doi.org/10.1016/j.ultsonch.2015.10.016.
[38] F. Touyeras, J.Y. Hihn, S. Delalande, R. Viennet, M.L. Doche, Ultrasound influence on the activation step before electroless coating, Ultrason. Sonochem. 10 (2003) 363–368, http://dx.doi.org/10.1016/S1350-4177(03)00098-1.
[39] L. Zhai, X. Liu, T. Li, Z. Feng, Z. Fan, Vacuum and ultrasonic co-assisted electroless copper plating on carbon foams, Vacuum 114 (2015) 21–25, http://dx.doi.org/10.1016/j.vacuum.2014.12.005.
[40] A.J. Cobley, T.J. Mason, V. Saez, Review of effect of ultrasound on electroless plating process, Trans. Inst. Met. Finish. (2011) 303–309, http://dx.doi.org/10.1179/174591911X13170500147670.
[41] X. Xu, Z.D. Cui, S.L. Zhu, Y.Q. Liang, X.J. Yang, Preparation of nickel-coated graphite by electroless plating under mechanical or ultrasonic agitation, Surf. Coatings Technol. 240 (2014) 425–431, http://dx.doi.org/10.1016/j.surfcoat.2013.12.070.

[42] A.J. Cobley, B. Abbas, A. Hussain, Improved electroless copper coverage at low catalyst concentrations and reduced plating temperatures enabled by low frequency ultrasound, Int. J. Electrochem. Sci. 9 (2014) 7795–7804.
[43] V. Niksefat, M. Ghorbani, Mechanical and electrochemical properties of ultrasonic-assisted electroless deposition of Ni-B-TiO_2 composite coatings, J. Alloys Compd. 633 (2015) 127–136, http://dx.doi.org/10.1016/j.jallcom.2015.01.250.
[44] I. Tudela, Y. Zhang, M. Pal, I. Kerr, A.J. Cobley, Ultrasound-assisted electrodeposition of thin nickel-based composite coatings with lubricant particles, Surf. Coatings Technol. 276 (2015) 89–105.
[45] J. Jiang, H. Lu, L. Zhang, N. Xu, Preparation of monodisperse Ni/PS spheres and hollow nickel spheres by ultrasonic electroless plating, Surf. Coatings Technol. 201 (2007) 7174–7179, http://dx.doi.org/10.1016/j.surfcoat.2007.01.031.
[46] D. Dong, X.H. Chen, W.T. Xiao, G.B. Yang, P.Y. Zhang, Preparation and properties of electroless Ni-P-SiO_2 composite coatings, Appl. Surf. Sci. 255 (2009) 7051–7055, http://dx.doi.org/10.1016/j.apsusc.2009.03.039.
[47] A. Agarwal, M. Pujari, R. Uppaluri, A. Verma, Efficacy of reducing agent and surfactant contacting pattern on the performance characteristics of nickel electroless plating baths coupled with and without ultrasound, Ultrason. Sonochem. 21 (2014) 1382–1391, http://dx.doi.org/10.1016/j.ultsonch.2014.01.015.
[48] Z. Sharifalhoseini, M.H. Entezari, R. Jalal, Evaluation of antibacterial activity of anticorrosive electroless Ni-P coating against Escherichia coli and its enhancement by deposition of sono-synthesized ZnO nanoparticles, Surf. Coatings Technol. 266 (2015) 160–166, http://dx.doi.org/10.1016/j.surfcoat.2015.02.035.
[49] Y. de Hazan, D. Zimmermann, M. Z'graggen, S. Roos, C. Aneziris, H. Bollier, P. Fehr, T. Graule, Homogeneous electroless Ni-P/SiO_2 nanocomposite coatings with improved wear resistance and modified wear behavior, Surf. Coatings Technol. 204 (2010) 3464–3470, http://dx.doi.org/10.1016/j.surfcoat.2010.04.007.
[50] A. Chiba, H. Haijima, W.C. Wu, Effect of sonication on the electroless Ni-B deposited powder from acid bath, Ultrasonics 42 (2004) 617–620, http://dx.doi.org/10.1016/j.ultras.2004.01.084.
[51] Q.L. Rao, G. Bi, Q.H. Lu, H.W. Wang, X.L. Fan, Microstructure evolution of electroless Ni-B film during its depositing process, Appl. Surf. Sci. 240 (2005) 28–33, http://dx.doi.org/10.1016/j.apsusc.2004.07.059.
[52] I. Apachitei, J. Duszczyk, Hydrogen evolution, incorporation and removal in electroless nickel composite coatings on aluminium, J. Appl. Electrochem. 29 (1999) 835–841, http://dx.doi.org/10.1023/A:1003526709182.
[53] H. Yanagida, The effect of dissolve gas concentration in the initial growth stage of multi cavitation bubbles. Differences between vacuum degassing and ultrasound degassing, Ultrason. Sonochem. 15 (2008) 492–496, http://dx.doi.org/10.1016/j.ultsonch.2007.06.008.
[54] R. Weil, K. Parker, The properties of electroless nickel, Electroless Plat. (1990) 111–137, <www.knovel.com>.
[55] Z.C. Wang, L. Yu, Z.B. Qi, G.L. Song, Electroless nickel-boron plating to improve the corrosion resistance of magnesium (Mg) alloys, Corros. Prev. Magnes. Alloy. (2013) 370–392, http://dx.doi.org/10.1533/9780857098962.3.370.
[56] M. Sribalaji, P. Arunkumar, K.S. Babu, A.K. Keshri, Crystallization mechanism and corrosion property of electroless nickel phosphorus coating during intermediate temperature oxidation, Appl. Surf. Sci. 355 (2015) 112–120, http://dx.doi.org/10.1016/j.apsusc.2015.07.061.
[57] D.V.V. Moll, R.C. Salvarezza, H.A. Videla, A.J. Arvia, The pitting corrosion of nickel in different electrolyte solutions containing chloride ions, (1900).